Dinuclear and Hexanuclear Iron(III) Oxide Complexes with a Bis(bipyridine) Ligand: A New $[Fe_6(\mu_3\text{-}O)_4]^{10+}$ Core

Craig M. Grant,[1a] Michael J. Knapp,[1b] William E. Streib,[1a] John C. Huffman,[1a] David N. Hendrickson,*[,1b] and George Christou*[,1a]

Department of Chemistry and Molecular Structure Center, Indiana University, Bloomington, Indiana 47405-4001, and Department of Chemistry, University of California at San Diego, La Jolla, California 92093-0358

Received June 18, 1998

The use of the bis(bipyridine) ligand L (1,2-bis(2,2′-bipyridyl-6-yl)ethane) has yielded new dinuclear and hexanuclear complexes. The $FeCl_3/NaO_2CPh/L$ (4:4:1) reaction system in MeCN gives red-brown $[Fe_6O_4Cl_4(O_2CPh)_4L_2][FeCl_4]_2$ (**1**). The same reaction system in a 3:3:1 ratio in MeOH gives orange $[Fe_2(OMe)_2Cl_2(O_2CPh)L][FeCl_4]$ (**2**). Complex **1**·2MeCN: monoclinic, $P2_1/a$, $a = 15.317(2)$ Å, $b = 18.303(3)$ Å, $c = 16.168(3)$ Å, $\beta = 108.91(1)°$, and $Z = 2$. Complex **2**: triclinic, $P\bar{1}$, $a = 14.099(6)$ Å, $b = 18.510(7)$ Å, $c = 7.108(3)$ Å, $\alpha = 96.77(2)°$, $\beta = 99.45(2)°$, $\gamma = 81.16(2)°$, and $Z = 2$. The cation of **1** consists of a near-planar $[Fe_6(\mu_3\text{-}O)_4]^{10+}$ core that can be described as three edge-fused $[Fe_2O_2]$ rhombs to which are attached two additional Fe atoms. The cation of **2** contains a $[Fe_2(\mu\text{-}OMe)_2(\mu\text{-}O_2CPh)]^{3+}$ core. In both cations, the L group acts as a bridging ligand across an Fe_2 unit, with the bpy rings essentially parallel. Variable-temperature solid-state magnetic-susceptibility studies of **1** and **2** in the 2.00−300 K range reveal that for both complexes the data are consistent with an $S = 0$ cation and $S = {}^5/_2$ $[FeCl_4]^-$ anions. These conclusions were confirmed by magnetization vs field studies in the 2.00−4.00 K and 10.0−50.0 kG ranges. Fitting of the data for **2** to the appropriate theoretical equation for an equimolar composition of Fe_2 cations and $[FeCl_4]^-$ anions allowed the exchange interaction in the cation to be determined as $J = -10.5$ cm^{-1} ($H = -2JS_1S_2$) with g held at 2.00. The obtained J value is consistent with that predicted by a previously published magnetostructural relationship.

Introduction

The systematic development of 3d metal carboxylate cluster chemistry over the last dozen years or so has led to a remarkable variety of species that have been of interest from several viewpoints, including structural aesthetics and spectroscopic and physical properties.[2−5] For Fe and Mn, in particular, this area has, for example, been the source of discrete species with large (and sometimes abnormally large) values of ground-state spin (S).[2−5] In some cases, a large S value in combination with significant magnetoanisotropy has resulted in some species being magnetizable magnets.[6−10] This new magnetic phenomenon, which we have termed single-molecule magnetism,[9a] represents an exciting development within the general field of nanoscale magnets (nanomagnets).

The future health of the field of high spin molecules and the chances of identifying new single-molecule magnets will both benefit from the development of new synthesis methodologies to 3d metal clusters. With this in mind, we have been exploring the use of, among others, the bis(bipyridine) ligand L (1,2-bis-(2,2′-bipyridyl-6-yl)ethane) with the belief that it might foster formation of discrete polynuclear metal systems. Recently, we

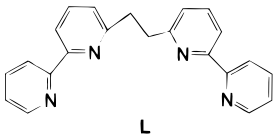

L

reported, for example, that it gives an octanuclear mixed-valence $4Co^{II},4Co^{III}$ cluster $[Co_8O_4(OH)_4(O_2CMe)_6L_2](ClO_4)_2$.[11] Here we describe its use to prepare new Fe_2 and Fe_6 species, which we believe to be the first in a series of new Fe_x^{III} and Mn_x^{III} clusters.

(1) (a) Indiana University. (b) University of California at San Diego.
(2) Christou, G. in *Magnetism: A Supramolecular Function*; Kahn, O., Ed.; NATO ASI Series; Kluwer: Dordrecht, 1996.
(3) Gatteschi, D.; Caneschi, A.; Sessoli, R.; Cornia, A. *Chem. Soc. Rev.* **1996**, *25*, 101.
(4) Winpenny, R. E. P. *Acc. Chem. Res.* **1997**, *30*, 89.
(5) Aromí, G.; Aubin, S. M. J.; Bolcar, M. A.; Christou, G.; Eppley, H. J.; Folting, K.; Hendrickson, D. N.; Huffman, J. C.; Squire, R. C.; Tsai, H.-L.; Wang, S.; Wemple, M. W. *Polyhedron* **1998**, *17*, 3005.
(6) (a) Sessoli, R.; Tsai, H.-L.; Schake, A. R.; Wang, S.; Vincent, J. B.; Folting, K.; Gatteschi, D.; Christou, G.; Hendrickson, D. N. *J. Am. Chem. Soc.* **1993**, *115*, 1804. (b) Sessoli, R.; Gatteschi, D.; Caneschi, A.; Novak, M. *Nature* **1993**, *365*, 141.
(7) (a) Eppley, H. J.; Tsai, H.-L.; DeVries, N.; Folting, K.; Christou, G.; Hendrickson, D. N. *J. Am. Chem. Soc.* **1995**, *117*, 301. (b) Aubin, S. M. J.; Spagna, S.; Eppley, H. J.; Sager, R. E.; Christou, G.; Hendrickson, D. N. *Chem. Commun.* **1998**, 803.
(8) Aubin, S. M. J.; Eppley, H. J.; Guzei, I. A.; Folting, K.; Grantzel, P. K.; Rheingold, A. L.; Christou, G.; Hendrickson, D. N. *J. Am. Chem. Soc.*, submitted for publication.
(9) (a) Aubin, S. M. J.; Wemple, M. W.; Adams, D. M.; Tsai, H.-L.; Christou, G.; Hendrickson, D. N. *J. Am. Chem. Soc.* **1996**, *118*, 7746. (b) Aubin, S. M. J.; Dilley, N. R.; Pardi, L.; Krzystek, J.; Wemple, M. W.; Brunel, I.-C.; Maple, M. B.; Christou, G.; Hendrickson, D. N. *J. Am. Chem. Soc.* **1998**, *120*, 4991.
(10) (a) Sun, Z.; Grant, C. M.; Castro, S. L.; Hendrickson, D. N.; Christou, G. *Chem. Commun.* **1998**, 721. (b) Castro, S. L.; Sun, Z.; Grant, C. M.; Bollinger, J. C.; Hendrickson, D. N.; Christou, G. *J. Am. Chem. Soc.* **1998**, *120*, 2365.
(11) Grillo, V. A.; Sun, Z.; Folting, K.; Hendrickson, D. N.; Christou, G. *Chem. Commun.* **1996**, 2233.

10.1021/ic980686k CCC: $15.00
Published on Web 10/31/1998

Experimental Section

Syntheses. All manipulations were carried out under aerobic conditions using materials as received. The bis(bipyridine) ligand L was synthesized as described elsewhere.[12]

$[Fe_6O_4Cl_4(O_2CPh)_4L_2][FeCl_4]_2$ (1). A solution of $FeCl_3$ (0.174 g, 1.07 mmol) and NaO_2CPh (0.155 g, 1.07 mmol) in MeCN (25 mL) was treated with L (0.091 g, 0.269 mmol) and left overnight at room temperature. The resultant red-brown solution was filtered to remove NaCl, and the filtrate volume was reduced by half. Layering with Et_2O led to the slow formation of red-brown crystals of **1**·2MeCN over 1−2 weeks. These were collected by filtration, washed with Et_2O, and dried in vacuo. The yield was ∼40% (∼0.11 g). The crystallographic sample was maintained in contact with mother liquor to avoid solvent loss. The dried sample was analyzed as **1**·MeCN. Anal. Calcd (found) for $C_{74}H_{59}Cl_{12}Fe_8N_9O_{12}$: C, 41.56 (41.34); H, 2.78 (2.71); N, 5.89 (5.68). Selected IR data (KBr, cm^{-1}): 1601 (vs), 1574 (s), 1508 (vs), 1454 (vs), 1400 (vs), 1309 (m), 1302 (m), 1169 (m), 1024 (vs), 777 (vs), 721 (vs), 686 (s), 677 (s), 640 (vs), 464 (s).

$[Fe_2(OMe)_2Cl_2(O_2CPh)L][FeCl_4]$ (2). Na_2OCPh (0.159 g, 1.11 mmol) was dissolved in a solution of $FeCl_3$ (0.180 g, 1.11 mmol) in MeOH (20 mL) to give a yellow-orange solution. To this was added a warm solution of L (0.122 g, 0.362 mmol) in MeOH (20 mL), causing the rapid formation of an orange precipitate. The solid was collected by filtration, washed with MeOH, and dried in vacuo. The yield was 78% (0.26 g). The orange solid was recrystallized from boiling MeOH/MeCN (10 mL:10 mL), and the resultant orange solution was allowed to stand and to become concentrated by evaporation. Orange needles began to form after 2−3 days and were collected by filtration after 2 weeks; the yield was 28% (0.09 g). The dried solid was analyzed as solvent-free. Anal. Calcd (found) for $C_{31}H_{29}Cl_6Fe_3N_4O_4$: C, 41.29 (41.36); H, 3.24 (3.28); N, 6.21 (6.24). Selected IR data (KBr, cm^{-1}): 1601 (vs), 1574 (w), 1566 (w), 1516 (vs), 1493 (s), 1454 (vs), 1412 (vs), 1402 (vs), 1307 (m), 1165 (m), 1020 (vs), 1012 (vs), 779 (vs), 717 (s), 680 (m), 640 (m).

X-ray Crystallography. Data were collected using a Picker four-circle diffractometer; details of the diffractometry, low-temperature facilities, and computational procedures employed by the Molecular Structure Center are available elsewhere.[13a] Suitable crystals were located, affixed to glass fibers using silicone grease, and then transferred to a goniostat, where they were cooled for characterization and data collection. The structures were solved by direct methods (MULTAN or SHELXTL) and standard Fourier techniques and refined on F by full-matrix least-squares cycles.

For complex **1**·2MeCN, a systematic search of a limited hemisphere of reciprocal space revealed a primitive monoclinic cell. On the basis of intensity data collection ($+h, +k, \pm l$; $6 \le 2\theta \le 50°$), the conditions $h = 2n$ for $h01$ and $k = 2n$ for $0k0$ uniquely determined the space group as $P2_1/a$. After an analytical correction for absorption using the Program AGNOST,[13b] data processing produced a unique set of 7564 intensities and an $R_{av} = 0.031$ for the averaging of 2870 of the intensities which had been observed more than once. Four standards measured every 300 reflections showed no significant trends. All non-hydrogen atoms were located without problems and refined anisotropically. Hydrogen atoms were included in fixed, calculated positions with thermal parameters fixed at one plus the isotropic thermal parameter of the parent atom. All of the unique data were used; however, data with $F < 3\sigma(F)$ were given zero weight. The largest peak in the final difference Fourier map was 0.68 e/Å^3, located 1.1 Å from Cl(55) of the anion, and the deepest hole was −0.54 e/Å^3.

For complex **2**, a systematic search of a limited hemisphere of reciprocal space revealed no symmetry or systematic absences, which indicated a triclinic space group. Subsequent solution and refinement confirmed the centrosymmetric choice $P\bar{1}$. All non-hydrogen atoms were readily located without problem and refined anisotropically. Hydrogen atoms were included in the final refinement cycles in fixed, calculated positions with thermal parameters fixed at one plus the isotropic thermal parameter of the parent atom. A final difference Fourier map was featureless, and the largest peak was 0.62 e/Å^3.

Final crystallographic data and values of $R(F)$ and $R_w(F)$ are listed in Table 1.

Table 1. Crystallographic Data for Complexes **1**·2MeCN and **2**

	1·2MeCN	**2**
formula[a]	$C_{76}H_{62}Cl_{12}Fe_8N_{10}O_{12}$	$C_{31}H_{29}Cl_6Fe_3N_4O_4$
formula wt. g/mol	2179.60	901.85
space group	$P2_1/a$	$P\bar{1}$
a, Å	15.317(2)	14.099(6)
b, Å	18.303(3)	18.510(7)
c, Å	16.168(3)	7.108(3)
α, deg	90	96.77(2)
β, deg	108.91(1)	99.45(2)
γ, deg	90	81.16(2)
V, Å^3	4288.1	1800.0
Z	2	2
T, °C	−169	−172
radiation,[b] Å	0.71069	0.71069
ρ_{calc}, g/cm^3	1.688	1.664
μ, cm^{-1}	17.498	16.784
R (R_w),[c,d] %	5.51 (5.76)	5.58 (4.31)

[a] Including solvate molecules. [b] Mo Kα, graphite monochromator. [c] $R = 100\sum||F_o| - |F_c||/\sum|F_o|$. [d] $R_w = 100[\sum w(|F_o| - |F_c|)^2/\sum w|F_o|^2]^{1/2}$ where $w = 1/\sigma^2(|F_o|)$.

Physical Measurements. IR and electronic spectra were recorded on KBr disks and solutions, respectively, on Nicolet model 510P and Hewlett Packard model 8452A spectrophotometers, respectively. DC magnetic-susceptibility data were collected on powdered, microcrystalline samples (restrained in eicosane to prevent torquing) on a Quantum Design MPMS5 SQUID magnetometer equipped with a 5.5 T (55 kG) magnet. A diamagnetic correction to the observed susceptibilities was applied using Pascal's constants.

Results

Syntheses. Our initial use of the bis(bipyridine) ligand L in metal carboxylate chemistry had been in the reaction with $[Mn_3O(O_2CMe)_6(py)_3](ClO_4)$, which had led to formation of tetranuclear $[Mn_4O_2(O_2CMe)_4L_2](ClO_4)_2$ (**3**) containing $2Mn^{II}$ and $2Mn^{III}$ ions.[14] Through the extension of the use of L to Fe chemistry, the $FeCl_3/NaO_2CPh$/L reaction system in MeCN or MeOH was explored. The 4:4:1 reaction in MeCN yielded a red-brown solution from which was crystallized $[Fe_6O_4Cl_4(O_2CPh)_4L_2][FeCl_4]_2$·2MeCN (**1**·2MeCN) in 40% yield on layering with Et_2O. The preparation may be summarized as in eq 1, based on the reasonable assumption that H_2O is the source of the O^{2-} ions. Thus, the "excess" Fe over that required for

$$8FeCl_3 + 8NaO_2CPh + 2L + 4H_2O \rightarrow [Fe_6O_4Cl_4(O_2CPh)_4L_2][FeCl_4]_2 + 8NaCl + 4PhCO_2H + 4HCl \quad (1)$$

formation of the Fe_6 cation provides $[FeCl_4]^-$ anions.

A related reaction with an $FeCl_3/NaO_2CPh$/L ratio of 3:3:1 but in MeOH instead of MeCN rapidly gives an orange powder that was recrystallized from MeOH/MeCN and identified as $[Fe_2(OMe)_2Cl_2(O_2CPh)L][FeCl_4]$ (**2**). Its formation is summarized in eq 2. The same product is also obtained if the red-

$$3FeCl_3 + 3NaO_2CPh + L + 2MeOH \rightarrow [Fe_2(OMe)_2Cl_2(O_2CPh)L][FeCl_4] + 3NaCl + 2PhCO_2H \quad (2)$$

(12) Garber, T.; Van Wallendael, S.; Rillema, D. P.; Kirk, M.; Hatfield, W. E.; Welch, J. H.; Singh, P. *Inorg. Chem.* **1990**, *29*, 2863.
(13) (a) Chisholm, M. H.; Folting, K.; Huffman, J. C.; Kirkpatrick, C. C. *Inorg. Chem.* **1984**, *23*, 1021. (b) de Meulenaer, J.; Tompa, H. *Acta Crystallogr.* **1965**, *19*, 1014.
(14) Grillo, V. A.; Knapp, M. J.; Bollinger, J. C.; Hendrickson, D. N.; Christou, G. *Angew. Chem., Int. Ed. Engl.* **1996**, *35*, 1818.

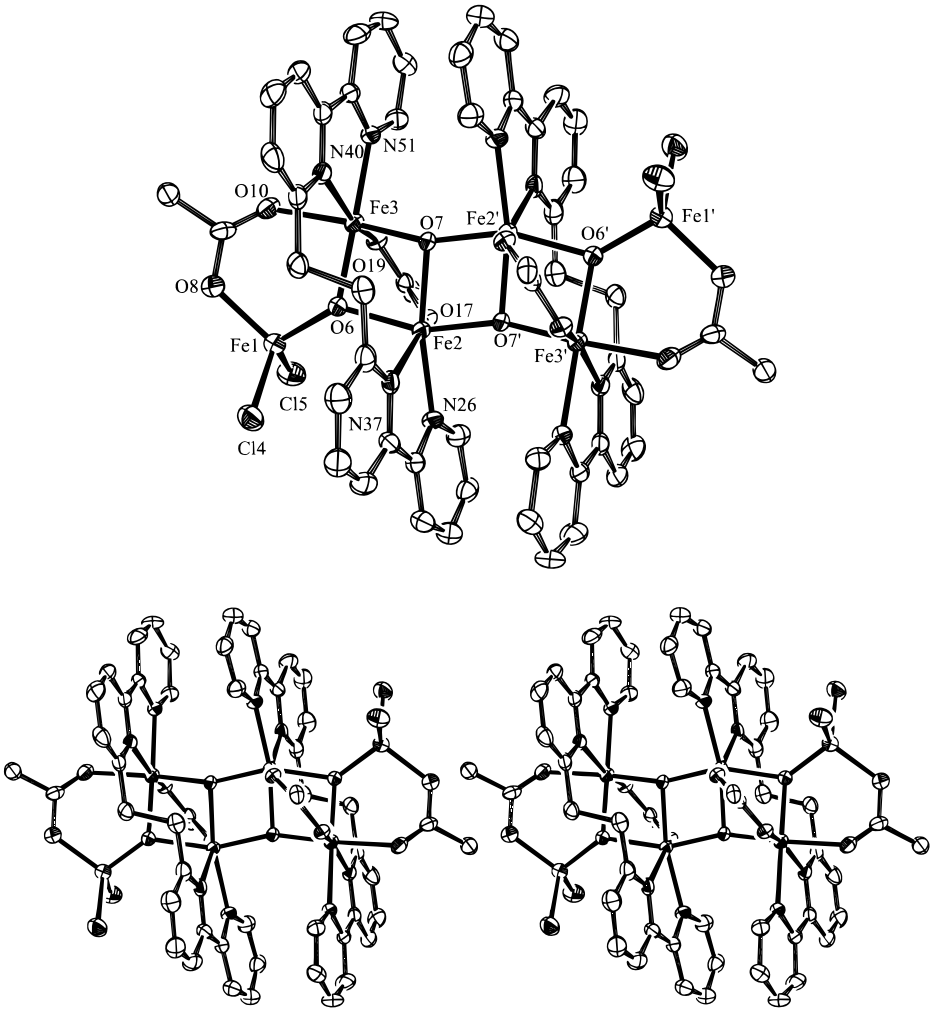

Figure 1. Labeled ORTEP plot showing 50% probability ellipsoids and a stereopair of the cation of complex **1**·2MeCN. Primed and unprimed atoms are related by the center of inversion.

brown (4:4:1) reaction solution of **1** is concentrated under vacuum, the residue extracted with boiling MeOH/MeCN, and the resulting orange solution allowed to slowly evaporate. Thus, the cation of complex **1** undergoes a methanolysis to give the cation of **2**; the structure of the latter is, in fact, related to that of **1** even though the nuclearities are so different (vide infra).

Description of Structures. ORTEP diagrams of the cations of **1** and **2** are provided in Figures 1−4, and selected interatomic distances and angles are listed in Tables 2 and 3.

Complex **1** crystallizes in monoclinic space group $P2_1/a$, with the Fe_6 cation lying on a center of inversion. The $[FeCl_4]^-$ anions are unexceptional, with tetrahedral geometry and Fe−Cl distances of ∼2.2 Å. The centrosymmetric cation contains an unusual $[Fe_6(\mu_3\text{-}O)_4]^{10+}$ core ($6Fe^{III}$) that can be conveniently described as consisting of three edge-fused $[Fe_2O_2]$ rhombs to which are attached two additional Fe atoms Fe(1) and Fe(1′). The latter are four-coordinate with distorted tetrahedral geometry whereas the other Fe atoms are six-coordinate with distorted octahedral geometry. This $[Fe_6O_4]^{10+}$ core is essentially planar, as emphasized by the side view presented in Figure 2. The greatest deviation from the Fe_6 least-squares plane is 0.11 Å by Fe(2) and Fe(2′), and O(6) and O(7) are 0.26 and 0.12 Å, respectively, out of the bridged Fe_3 planes. Whereas O(6) is distorted trigonal planar, O(7) is nearly *T*-shaped, with the Fe(2′)-O(7)−Fe(3) angle being 159.25(21)° (Figure 3). Fe···Fe separations bridged by two O^{2-} ions are significantly shorter (∼3.0 Å) than those bridged by one O^{2-} ion (∼3.4−3.5 Å). All core distances and angles are conveniently indicated in Figure 3. Peripheral ligation is provided by terminal Cl^- and bridging $PhCO_2^-$ and L groups, with the latter in a chelating and bridging mode. The overall cation has C_i symmetry. The $[Fe_6O_4]^{10+}$ core has not been previously seen for either Fe^{III} or Mn^{III}, although the Fe_6 dispositions are somewhat similar to the Mn_6 dispositions in $[Mn_6O_2(OMe)_6(O_2CMe)_2(L')_2]$, where

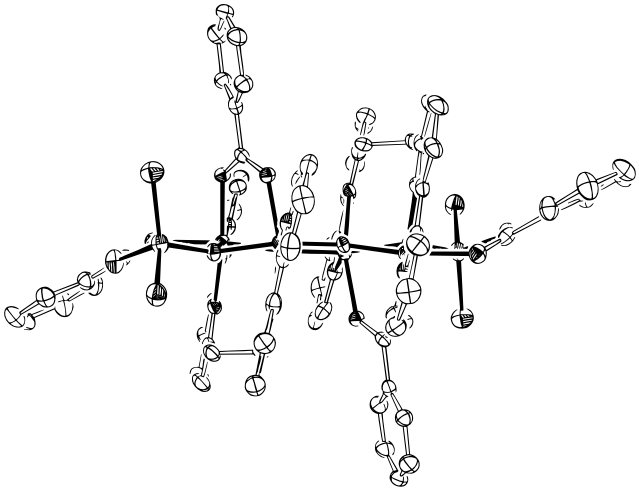

Figure 2. Side view of the cation of complex **1**·2MeCN emphasizing the near planarity of the $[Fe_6O_4]$ core.

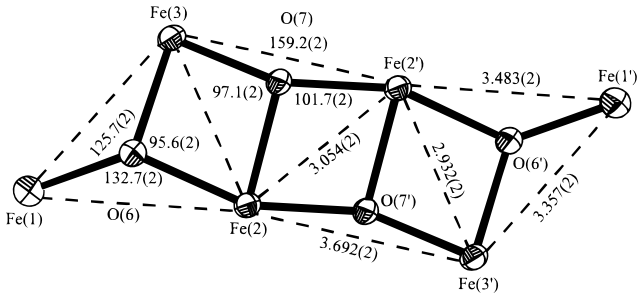

Figure 3. [Fe_6O_4] core of the cation of complex **1**·2MeCN showing interatomic distances and angles.

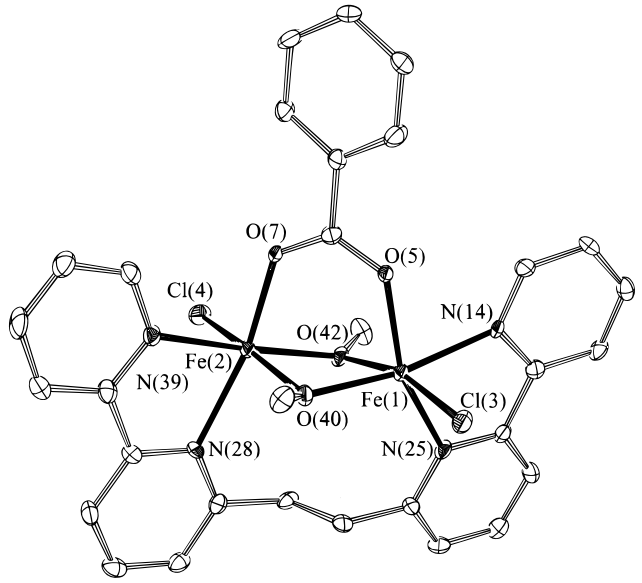

Figure 4. Labeled ORTEP plot showing 50% probability ellipsoids of the cation of complex **2**.

L′ is a pentadentate Schiff base ligand, which contains a $[Mn_6(\mu_3\text{-}O)_2(\mu_3\text{-}OMe)_2]^{10+}$ core with additional μ-OMe bridges on the periphery;[15] the μ_3-OMe groups are pyramidal rather than planar. There are now several different structural types in Fe_6 cluster chemistry, including Fe_6 octahedra,[16] Fe_6 hexagons,[17] and more extended Fe_6 units that can be described as two linked Fe_3 triangular units.[18]

There are several alternative ways of describing the structure of the cation of **1**, but the following is particularly useful: the cation consists of two $[Fe_2O_2(O_2CPh)L]^+$ fragments that are linked by interfragment bonds Fe(2)−O(7′) and Fe(2′)−O(7), and this incipient, supramolecular chain formation is terminated by the $[FeCl_2(O_2CPh)]$ caps at each end, whose Fe(1) and O(10) atoms bind to and prevent O(6) and Fe(3) from attaching to

(15) Xia, X.; Verelst, M.; Daran, J.-C.; Tuchagues, J.-P. *J. Chem. Soc., Chem. Commun.* **1995**, 2155.

(16) (a) Brechin, E.; Knapp, M. J.; Huffman, J. C.; Hendrickson, D. N.; Christou, G. *Inorg. Chem.*, submitted for publication. (b) Hegetschweiler, K.; Schmalle, H. W.; Streit, H. M.; Gramlich, V.; Hund, H.-U.; Erni, I. *Inorg. Chem.* **1992**, *31*, 1299. (c) Cornia, A.; Gatteschi, D.; Hegetschwiler, K.; Hausherr-Primo, L.; Gramlich, V. *Inorg. Chem.* **1966**, *35*, 4414.

(17) (a) Tokii, T.; Ide, K.; Nakashima, M.; Koikawa, M. *Chem. Lett.* **1994**, 441. (b) Caneschi, A.; Cornia, A.; Lippard, S. J. *Angew. Chem., Int. Ed. Engl.* **1995**, *34*, 467.

(18) (a) Christmas, C. A.; Tsai, H.-L.; Pardi, L.; Kesselman, J. M.; Grantzel, P. K.; Chadha, R. K.; Gatteschi, D.; Harvey, D. F.; Hendrickson, D. N. *J. Am. Chem. Soc.* **1993**, *115*, 12483. (b) Nair, V. S.; Hagen, K. S. *Inorg. Chem.* **1992**, *31*, 4048. (c) Batsanov, A. S.; Struchkov, Y. T.; Timko, G. A. *Koord. Khim.* **1988**, *14*, 266. (d) Micklitz, W.; Bott, S. G.; Bentsen, J. G.; Lippard, S. J. *J. Am. Chem. Soc.* **1989**, *111*, 372. (e) Harding, C. J.; Henderson, R. K.; Powell, A. K. *Angew. Chem., Int. Ed. Engl.* **1993**, *32*, 570. (f) Chaudhuri, P.; Hess, M.; Rentschler, E.; Weyhermuller, T.; Florke, U. *New J. Chem.* **1998**, *22*, 553.

Table 2. Selected Interatomic Distances (Å) and Angles (deg) for Complex **1**·2MeCN

Fe(1)−Fe(2)	3.483(2)	Fe(2)−Fe(3)	2.932(2)
Fe(1)−Fe(3)	3.357(2)	Fe(2)−Fe(2′)	3.054(2)
Fe(1)−Cl(4)	2.191(2)	Fe(3)−O(6)	1.965(4)
Fe(1)−Cl(5)	2.199(2)	Fe(3)−O(7)	1.864(4)
Fe(1)−O(6)	1.806(4)	Fe(3)−O(10)	2.086(4)
Fe(1)−O(8)	1.939(4)	Fe(3)−O(19)	2.058(4)
Fe(2)−O(6)	1.994(4)	Fe(3)−N(40)	2.230(5)
Fe(2)−O(7′)	1.889(4)	Fe(3)−N(51)	2.140(5)
Fe(2)−O(7)	2.045(4)	Fe(52)−Cl(53)	2.197(2)
Fe(2)−O(17)	2.038(4)	Fe(52)−Cl(54)	2.199(2)
Fe(2)−N(26)	2.166(5)	Fe(52)−Cl(55)	2.187(3)
Fe(2)−N(37)	2.194(5)	Fe(52)−Cl(56)	2.193(2)
Cl(4)−Fe(1)−Cl(5)	110.52(8)	O(6)−Fe(2)−O(17)	86.32(16)
Cl(4)−Fe(1)−O(6)	108.21(13)	O(6)−Fe(2)−N(26)	110.90(17)
Cl(4)−Fe(1)−O(8)	108.02(14)	O(6)−Fe(2)−N(37)	85.67(16)
Cl(5)−Fe(1)−O(6)	112.39(14)	O(7)−Fe(2)−O(7)′	78.25(16)
Cl(5)−Fe(1)−O(8)	114.38(15)	O(7)′-Fe(2)−O(17)	100.31(16)
O(6)−Fe(1)−O(8)	102.89(17)	O(7)−Fe(2)−O(17)	90.40(15)
O(6)−Fe(2)−O(7)′	156.34(16)	O(7)′−Fe(2)−N(26)	92.57(17)
O(6)−Fe(2)−O(7)	79.02(15)	O(7)−Fe(2)−N(26)	167.06(17)
O(7)′−Fe(2)−N(37)	98.00(17)	O(7)−Fe(3)−N(51)	98.49(17)
O(7)−Fe(2)−N(37)	114.90(17)	O(10)−Fe(3)−O(19)	91.01(16)
O(17)−Fe(2)−N(26)	82.23(17)	O(10)−Fe(3)−N(40)	80.58(16)
O(17)−Fe(2)−N(37)	151.34(17)	O(10)−Fe(3)−N(51)	86.86(17)
N(26)−Fe(2)−N(37)	75.09(19)	O(19)−Fe(3)−N(40)	160.94(16)
O(6)−Fe(3)−O(7)	84.26(16)	O(19)−Fe(3)−N(51)	86.36(17)
O(6)−Fe(3)−O(10)	90.97(16)	N(40)−Fe(3)−N(51)	76.19(18)
O(6)−Fe(3)−O(19)	88.55(15)	Cl(53)−Fe(52)−Cl(54)	108.09(8)
O(6)−Fe(3)−N(40)	108.53(17)	Cl(53)−Fe(52)−Cl(55)	108.07(11)
O(6)−Fe(3)−N(51)	174.42(18)	Cl(53)−Fe(52)−Cl(56)	111.14(10)
O(7)−Fe(3)−O(10)	171.66(17)	Cl(54)−Fe(52)−Cl(55)	111.77(10)
O(7)−Fe(3)−O(19)	95.69(16)	Cl(54)−Fe(52)−Cl(56)	108.18(8)
O(7)−Fe(3)−N(40)	94.43(16)	Cl(55)−Fe(52)−Cl(56)	109.60(11)
Fe(1)−O(6)−Fe(2)	132.78(21)		
Fe(1)−O(6)−Fe(3)	125.69(20)		
Fe(2)−O(6)−Fe(3)	95.56(16)		
Fe(2)−O(7)−Fe(2)′	101.75(16)		
Fe(2)′−O(7)−Fe(3)	159.25(21)		
Fe(2)−O(7)−Fe(3)	97.09(16)		

Table 3. Selected Interatomic Distances (Å) and Angles (deg) for Complex **2**

Fe(1)−Fe(2)	3.088(2)	Fe(2)−O(40)	2.013(4)
Fe(1)−Cl(3)	2.290(2)	Fe(2)−O(42)	1.973(4)
Fe(1)−O(5)	2.014(4)	Fe(2)−N(28)	2.215(5)
Fe(1)−O(40)	1.981(4)	Fe(2)−N(39)	2.129(5)
Fe(1)−O(42)	1.993(4)	Fe(44)−Cl(45)	2.208(2)
Fe(1)−N(14)	2.176(5)	Fe(44)−Cl(46)	2.199(2)
Fe(1)−N(25)	2.219(5)	Fe(44)−Cl(47)	2.193(2)
Fe(2)−Cl(4)	2.271(2)	Fe(44)−Cl(48)	2.186(2)
Fe(2)−O(7)	2.042(4)		
Cl(3)−Fe(1)−O(5)	99.49(13)	O(40)−Fe(1)−N(25)	114.06(17)
Cl(3)−Fe(1)−O(40)	95.35(13)	O(42)−Fe(1)−N(14)	100.71(17)
Cl(3)−Fe(1)−O(42)	164.86(12)	O(42)−Fe(1)−N(25)	81.23(16)
Cl(3)−Fe(1)−N(14)	90.17(14)	N(14)−Fe(1)−N(25)	74.52(17)
Cl(3)−Fe(1)−N(25)	91.71(14)	Cl(4)−Fe(2)−O(7)	98.38(13)
O(5)− Fe(1)−O(40)	87.16(16)	Cl(4)−Fe(2)−O(40)	167.90(12)
O(5)− Fe(1)−O(42)	92.30(16)	Cl(4)−Fe(2)−O(42)	95.33(13)
O(5)− Fe(1)−N(14)	83.18(17)	Cl(4)−Fe(2)−N(28)	91.78(14)
O(5)− Fe(1)−N(25)	155.07(18)	Cl(4)−Fe(2)−N(39)	92.79(14)
O(40)−Fe(1)−O(42)	75.65(16)	O(7)−Fe(2)−O(40)	89.15(16)
O(40)−Fe(1)−N(14)	169.56(17)	O(7)−Fe(2)−O(42)	87.89(16)
O(7)−Fe(2)−N(28)	159.19(17)	N(28)−Fe(2)−N(39)	75.83(18)
O(7)−Fe(2)−N(39)	85.52(17)	Cl(45)−Fe(44)−Cl(46)	104.75(8)
O(40)−Fe(2)−O(42)	75.38(16)	Cl(45)−Fe(44)−Cl(47)	111.69(8)
O(40)−Fe(2)−N(28)	84.20(17)	Cl(45)−Fe(44)−Cl(48)	112.14(8)
O(40)−Fe(2)−N(39)	97.26(18)	Cl(46)−Fe(44)−Cl(47)	109.88(8)
O(42)−Fe(2)−N(28)	109.30(17)	Cl(46)−Fe(44)−Cl(48)	110.14(9)
O(42)−Fe(2)−N(39)	170.21(17)	Cl(47)−Fe(44)−Cl(48)	108.22(8)
Fe(1)−O(40)−Fe(2)	101.31(19)	Fe(1)−O(42)−Fe(2)	102.29(18)

another $[Fe_2O_2(O_2CPh)L]^+$ fragment. This is summarized below, where dashed lines indicate interfragment and capping bonds.

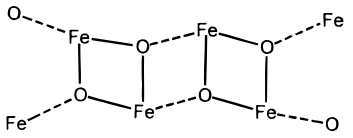

The chelating/bridging ligation mode adopted by the L group within an Fe_2 fragment aligns its two bpy halves parallel, and the interfragment linkage makes the two L groups parallel. This resulting parallel arrangement of the four bpy units is best seen in Figure 2. Thus, there appears to be no steric or other reason longer chains of $[Fe_2O_2(O_2CPh)L]^+$ repeating units with $[FeCl_2(O_2CPh)]$ caps at each end should not be possible, yielding the supramolecular $[Fe_{2n+2}O_{2n}Cl_4(O_2CPh)_{n+2}L_n]^{n+}$ family of which the cation of **1** is the $n = 2$ member; the core of the $[Fe_8O_6Cl_4(O_2CPh)_5L_3]^{3+}$ member with $n = 3$ is shown below. Such species may result from changes in reagent ratios, and this is under investigation.

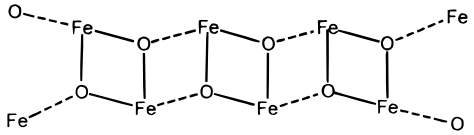

The cation of **2** (Figure 4) contains a $[Fe_2(\mu\text{-OMe})_2]^{4+}$ core with bridging L and $PhCO_2^-$ groups, with octahedral geometry at each Fe^{III} being completed by terminal Cl^- ions. The Fe···Fe distance is 3.088(2) Å and is similar to that in related dinuclear species; for example, the Fe···Fe distances in $[Fe_2(OR)_2Cl_2L'']$ are 3.097(7) and 3.115(7) Å (two independent molecules) when R = Me[19a] and 3.144(1) Å when R = Et[19b] (L″ = a hexadentate Schiff base ligand). Similarly, $[Fe_2(OEt)_2(acac)_4]$ has an Fe···Fe distance of 3.116(1) Å.[19b] The $[Fe_2(OMe)_2(O_2CR)]^{3+}$ core has apparently not been structurally characterized before in a dinuclear complex, although it is present in higher nuclearity species such as $[Fe_{10}(OMe)_{20}(O_2CR)_{10}]$ (R = Me,[20] CH_2Cl[21,22]), $[Fe_{12}O_2(OMe)_{18}(O_2CMe)_6(MeOH)_{4.67}]$,[23] and $[Fe_{18}(OH)_6(OMe)_{24}(O_2CMe)_{12}(XDK)_6]$[24] (XDK is a dicarboxylate).

A comparison between the cation of **2** and the $[Fe_2O_2(O_2CPh)L]^+$ fragment within **1** reveals that they are very similar. The L group in **2** adopts the same chelating/bridging mode, with four parallel bpy units and the $-CH_2CH_2-$ bridge lying on top of the central $[Fe_2O_2]$ rhomb and trans to the $PhCO_2^-$ group. Indeed, it is fairly accurate to say that the cation of **2** represents a $[Fe_2O_2(O_2CPh)L]^+$ fragment that has been stabilized to aggregation by methylation of the $\mu\text{-}O^{2-}$ bridges, with the resulting available coordination sites at the Fe^{III} atoms being occupied by Cl^- ions.

Magnetic-Susceptibility Studies. Solid-state, variable-temperature magnetic-susceptibility studies were carried out on powdered samples of complexes **1**·MeCN and **2** in the temperature range 2.00−300 K and an applied field of 10.0 kG (1 *T*). For complex **1**·MeCN, the μ_{eff} ($\chi_m T$) values slowly decrease from 10.21 (13.03) at 300 K to 8.23 (8.47) at 11.0 K and then decrease more rapidly to 6.70μ_B (5.61 cm^3 K mol^{-1}) at 2.00 K (Figure 5). Given that complex **1** comprises well-separated cations and $[FeCl_4]^-$ anions and that the latter are expected to be $S = {}^5/_2$ paramagnets, the 11.00 K values are similar to the spin-only values of 8.37 (8.76) expected for an $S = 0$ cation and two $S = {}^5/_2$ anions. The decrease at temperatures below 11 K is then likely due to zero-field splitting (ZFS) within the $S = {}^5/_2$ anions and perhaps some weak intermolecular antiferromagnetic interactions. To confirm the nature of the ground state of the Fe_6 cation, magnetization vs field data were collected in the 2.00−4.00 K range at fields of 10.0−50.0 kG. The data are presented as $M/N\mu_B$ vs H/T plots in Figure 6. Near-saturation is observed at a $M/N\mu_B$ value of ∼10, which is what is expected for an $S = 0$ cation and two $S = {}^5/_2$ anions with $g \approx 2.0$.

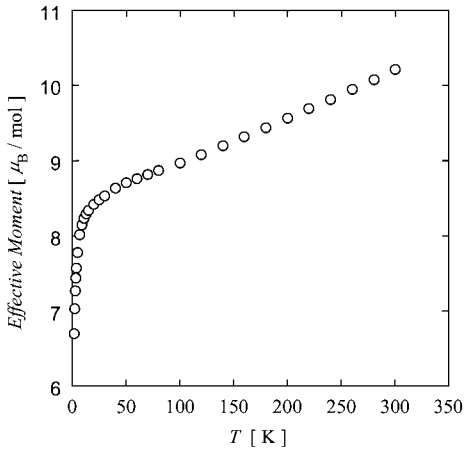

Figure 5. Plot of effective magnetic moment (μ_{eff}) vs *T* for complex **1**·MeCN in an applied field of 10.0 kG.

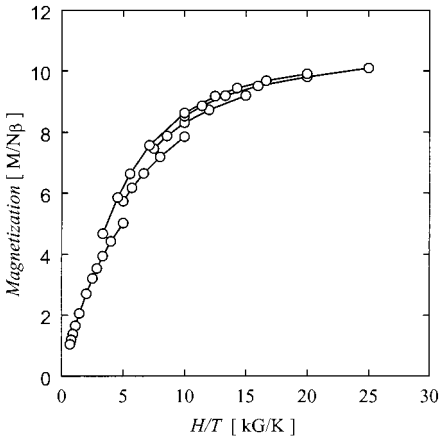

Figure 6. Plot of reduced magnetization ($M/N\mu_B$) vs H/T for complex **1**·MeCN in applied fields of 10.0, 20.0, 30.0, 40.0, and 50.0 kG. The solid lines are visual aids.

The $S = 0$ ground state of the Fe_6 cation is not surprising. This is a very common ground-state spin value for Fe_x^{III} clusters when x is an even number.[3,4,20,24] It should be noted that the $[Fe_6(\mu_3\text{-}O)_4]^{10+}$ core can also be considered as two $[Fe_4(\mu_3\text{-}O)_2]^{8+}$ units fused at the common Fe(2)−Fe(2′) edge. Such $[Fe_4O_2]^{8+}$ units with a planar or butterfly disposition of four Fe^{III} ions have previously been found to have an overall $S = 0$ ground state resulting from the individual $S = {}^5/_2$ spin alignments

(19) (a) Chiari, B.; Piovesana, O.; Tarantelli, T.; Zanazzi, P. F. *Inorg. Chem.* **1982**, *21*, 1396. (b) Chiari, B.; Piovesana, O.; Tarantelli, T.; Zanazzi, P. F. *Inorg. Chem.* **1984**, *23*, 3398.
(20) Benelli, C.; Parsons, S.; Solan, G. A.; Winpenny, R. E. P. *Angew. Chem., Int. Ed. Engl.* **1996**, *35*, 1825.
(21) Taft, K. L.; Lippard, S. J. *J. Am. Chem. Soc.* **1990**, *112*, 9629.
(22) Taft, K. L.; Delfs, C. D.; Papaefthymiou, G. C.; Foner, S.; Gatteschi, D.; Lippard, S. J. *J. Am. Chem. Soc.* **1994**, *116*, 823.
(23) Taft, K. L.; Papaefthymiou, G. C.; Lippard, S. J. *Inorg. Chem.* **1994**, *33*, 1510.
(24) Watton, S. P.; Fuhrmann, P.; Pence, L. E.; Caneschi, A.; Cornia, A.; Abbati, G. L.; Lippard, S. J. *Angew. Chem., Int. Ed. Engl.* **1997**, *36*, 2774.

shown.[25−29] Although the individual pairwise exchange interactions in the cation of **1** are not available and are not easily obtained for this particular cluster nuclearity and topology, they are likely to be similar to those in the $[Fe_4O_2]$ species because, in both cases, all Fe_2 pairs possess either one or two μ_3-O^{2-} bridges. As a result, a spin alignment pattern comparable to

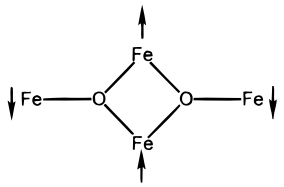

$[Fe_4O_2]^{8+}$

that above is likely but will be extended over the $[Fe_6O_4]^{10+}$ core as shown; this predicts an $S = 0$ ground state, as found experimentally.

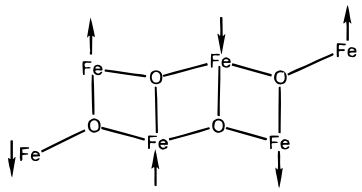

$[Fe_6O_4]^{10+}$

For complex **2**, $\mu_{eff}(\chi_m T)$ values steadily decrease from 9.33 (10.88) at 300 K to 6.02 (4.53) at 13.0 K and then more rapidly to $5.19\mu_B$ (3.37 cm^3 K mol^{-1}) at 2.00 K. The 13.0 K values are similar to the spin-only values of 5.92 (4.38) expected for an $S = {}^5/_2$ paramagnet, suggesting, therefore, that complex **2** comprises an $S = 0$ cation and an $S = {}^5/_2$ $[FeCl_4]^-$ anion. As for **1**, the decrease in $\mu_{eff}(\chi_m T)$ values below 13.0 K is likely due to ZFS within the $S = {}^5/_2$ anion or to weak intermolecular interactions. The μ_{eff} vs T data for the 13.0−300 K range were fit to the theoretical equation derived for a Heisenberg exchange model ($H = 2JS_1S_2$) with $S_1 = S_2 = {}^5/_2$ and including the contribution for an equimolar $S = {}^5/_2$ paramagnetic anion. The χ_m vs T equation for an exchange-coupled Fe_2^{III} system is given elsewhere;[30] converting it to μ_{eff} and incorporating the contribution of the $S = {}^5/_2$ anion gives the expression in eq 3 which was used to fit the experimental μ_{eff} vs T data. The fit (shown

$$\mu_{eff} = 2.828[\chi_m T + 4.38]^{1/2} \quad (3)$$

as the solid line in Figure 7) gives $J = -10.5$ cm^{-1} with g held constant at 2.00. The cation is thus antiferromagnetically coupled with an $S = 0$ ground state. The latter was confirmed by a $M/N\mu_B$ vs H/T plot (not shown) using data collected in the 2.00−4.00 K and 10.0−50.0 kG ranges; the plot saturates at $M/N\mu_B \approx 5$, consistent with an $S = 0$ cation and $S = {}^5/_2$ anion.

The J value for the cation is as expected from the empirical J vs P relationship reported by Gorun and Lippard,[31] where P is defined as half the shortest superexchange pathway between two Fe^{III} ions. The J vs P relationship is described by eq 4, where $A = 8.763 \times 10^{11}$, $B = -12.663$, and J is based on the $H = -2JS_iS_j$ spin Hamiltonian. In the cation of **2**, the Fe(1)−O(40)−Fe(2) and Fe(1)−O(42)−Fe(2) pathways have distances of 3.994(4) and 3.966(4) Å, respectively. Taking P as half the latter distance (1.983 Å) gives a predicted J of -10.9 cm^{-1}. Taking P as half the average of the two pathways (1.990 Å) gives $J = -10.0$ cm^{-1}. Both these predicted values are close to the experimental value of $J = -10.5$ cm^{-1}, which has an uncertainty of approximately ±5%.

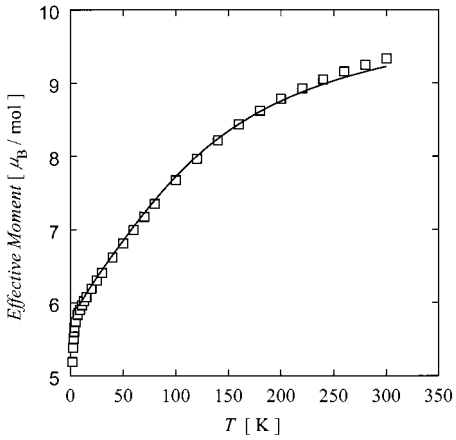

Figure 7. Plot of effective magnetic moment (μ_{eff}) vs T for complex **2**. The solid line is a fit of 13.0−300 K data to the appropriate theoretical equation. See the text for the fitting parameters.

$$-J = A \exp(BP) \quad (4)$$

Conclusions

The initial use of the bis(bipyridyl) ligand L in Fe^{III} carboxylate chemistry has provided access to two new Fe_x complexes, one dinuclear with a $[Fe_2(\mu\text{-OMe})_2(\mu\text{-}O_2CPh)]^{3+}$ core and the other hexanuclear with an unprecedented $[Fe_6(\mu_3\text{-}O)_4]^{10+}$ core. In both cases, the L ligand chelates and bridges an Fe_2 pair and thus acts as a binucleating ligand. It should be added that L has been previously shown by others to be capable of acting as a tetradentate ligand to a single metal ion,[12] so the bridging mode observed here attests to the flexibility of this ligand. Although both complexes have been found to possess $S = 0$ ground states, they nevertheless suggest possibilities for other Fe_x species that might exist and which may or may not have high-spin ground states. In addition, they provide encouragement for believing that a variety of Mn_x^{III} clusters should also be accessible with this ligand; such species will be interesting to study because in Mn_x^{III} cluster chemistry $S = 0$ or $S = {}^1/_2$ ground states are more the exception than the rule. Further work with Fe^{III} and parallel studies with Mn^{III} are currently in progress.

Acknowledgment. This work was supported by National Science Foundation grants to G.C. and D.N.H.

Supporting Information Available: Textual and tabular summaries of the structure determinations, tables of atomic coordinates, thermal parameters, and bond distances and angles, and fully labeled figures for complexes **1** and **2** (32 pages). Ordering information is given on any current masthead page.

IC980686K

(25) McCusker, J. K.; Vincent, J. B.; Schmitt, E. A.; Mino, M. L.; Shin, K.; Coggin, D. K.; Hagen, P. M.; Huffman, J. C.; Christou, G.; Hendrickson, D. N. *J. Am. Chem. Soc.* **1991**, *113*, 3012.
(26) Armstrong, W. H.; Roth, M. E.; Lippard, S. J. *J. Am. Chem. Soc.* **1987**, *109*, 6318.
(27) Gorun, S. M.; Lippard, S. J. *Inorg. Chem.* **1988**, *27*, 149.
(28) Chaudhuri, P.; Winter, M.; Fleischhauer, P.; Haase, W.; Florke, U.; Haupt, H.-J. *Inorg. Chim. Acta* **1993**, *212*, 241.
(29) Wemple, M. W.; Coggin, D. K.; Vincent, J. B.; McCusker, J. K.; Streib, W. E.; Huffman, J. C.; Hendrickson, D. N.; Christou, G. *J. Chem. Soc., Dalton Trans.* **1998**, 719.
(30) O'Connor, C. J. *Prog. Inorg. Chem.* **1982**, *29*, 203.
(31) Gorun, S. M.; Lippard, S. J. *Inorg. Chem.* **1991**, *30*, 1625.